



## ■ BONE BIOLOGY

# Tert-butylhydroquinone attenuates osteoarthritis by protecting chondrocytes and inhibiting macrophage polarization

H. Zhang,  
J. Li,  
X. Xiang,  
B. Zhou,  
C. Zhao,  
Q. Wei,  
Y. Sun,  
J. Chen,  
B. Lai,  
Z. Luo,  
A. Li

From The First Affiliated Hospital of Guangzhou University of Traditional Chinese Medicine, Guangzhou, China

## Aims

Tert-butylhydroquinone (tBHQ) has been identified as an inhibitor of oxidative stress-induced injury and apoptosis in human neural stem cells. However, the role of tBHQ in osteoarthritis (OA) is unclear. This study was carried out to investigate the role of tBHQ in OA.

## Methods

OA animal model was induced by destabilization of the medial meniscus (DMM). Different concentrations of tBHQ (25 and 50 mg/kg) were intraperitoneally injected in ten-week-old female mice. Chondrocytes were isolated from articular cartilage of mice and treated with 5 ng/ml lipopolysaccharide (LPS) or 10 ng/ml interleukin 1 beta (IL-1 $\beta$ ) for 24 hours, and then treated with different concentrations of tBHQ (10, 20, and 40  $\mu$ M) for 12 hours. The expression levels of malondialdehyde (MDA) and superoxide dismutase (SOD) in blood were measured. The expression levels of interleukin 6 (IL-6), IL-1 $\beta$ , and tumour necrosis factor alpha (TNF- $\alpha$ ) leptin in plasma were measured using enzyme-linked immunosorbent assay (ELISA) kits. The expression of nuclear factor kappa-light-chain-enhancer of activated B cells (NF- $\kappa$ B) and mitogen-activated protein kinase (MAPK) signalling pathway proteins, and macrophage repolarization-related markers, were detected by western blot.

## Results

Tert-butylhydroquinone significantly attenuated cartilage destruction in DMM-induced mice in vivo. It demonstrated clear evidence of inhibiting IL-1 $\beta$ -induced chondrocyte apoptosis, inflammation, and differentiation defect in vitro. Meanwhile, tBHQ inhibited LPS-induced activation of NF- $\kappa$ B and MAPK signalling pathways, and also inhibited LPS-induced reactive oxygen species production and macrophages repolarization in vitro.

## Conclusion

Taken together, tBHQ might be a potential therapeutic strategy for protecting against OA development.

Cite this article: *Bone Joint Res* 2021;10(11):704–713.

Keywords: tBHQ, Osteoarthritis, Apoptosis

## Article focus

■ To explore the effect of tert-butylhydroquinone (tBHQ) on osteoarthritis (OA).

- tBHQ significantly inhibited interleukin 1 beta (IL-1 $\beta$ ) induced chondrocyte apoptosis, inflammation, and differentiation defect in vitro.
- tBHQ significantly inhibited LPS-induced reactive oxygen species production, macrophage repolarization, and the activation of NF- $\kappa$ B and MAPK signalling pathways in chondrocytes.

## Key messages

■ tBHQ effectively protected against destabilization of the medial meniscus (DMM)-induced cartilage destruction and inflammation in mice.

Correspondence should be sent to Jie Li; email: Lijzzz@163.com

doi: 10.1302/2046-3758.1011.BJR-2020-0242.R4

*Bone Joint Res* 2021;10(11):704–713.

## Strengths and limitations

- tBHQ could effectively alleviate OA development by protecting chondrocytes against apoptosis, inflammation, and differentiation defect.
- Whether tBHQ alleviated OA by inhibiting the NF- $\kappa$ B and MAPK signalling pathways and macrophage repolarization needs to be investigated in detail in future studies.

## Introduction

Osteoarthritis (OA) is a common degenerative disease that can affect articular cartilage, synovium, and subchondral bone, and it is a leading cause of disability among older adults.<sup>1</sup> OA affects approximately 240 million people worldwide, including approximately 10% of men and 18% of women population who are over 60 years of age.<sup>2</sup> The main therapeutic strategies for OA are alleviating pain, reducing stiffness, maintaining the functional capacities, and improving the quality of life of OA patients.<sup>3,4</sup> Due to the limited knowledge of the molecular mechanisms involved in OA development, effective treatment strategies to decelerate OA progression are still lacking.<sup>5</sup> Therefore, better understanding of the underlying mechanisms of the occurrence and development of OA can contribute to identify specific therapeutic targets for OA treatment.

Reactive oxygen species (ROS) are mainly produced by the mitochondrial respiratory chain in aerobic metabolism (oxidative phosphorylation) or nicotinamide adenine dinucleotide phosphate (NADPH) oxidase.<sup>6</sup> ROS has been reported to promote OA by disrupting homeostatic intracellular signalling.<sup>7</sup> The ROS level maintains at low concentrations in chondrocytes under normal conditions, which participates in various intracellular processes and regulates cartilage metabolism including modulating chondrocyte apoptosis, downstream gene expression, and cytokine production.<sup>8,9</sup> However, in chondrocytes during OA, ROS level is significantly increased,<sup>10</sup> and the production of antioxidant enzyme is significantly decreased.<sup>11</sup> In addition, ROS plays an important role in the pathophysiology of OA with the presence of lipid peroxidation products.<sup>12</sup>

Chondrocytes are the resident cells for articular cartilage and the dysfunction of chondrocyte may severely cause the failure of articular cartilage.<sup>13</sup> Besides, apoptosis, inflammation, and differentiation of chondrocytes play essential roles in the development of OA.<sup>14</sup> In addition, macrophages actively participate in the pathophysiological processes of various chronic bone diseases such as gouty arthritis (GA), rheumatoid arthritis (RA), and OA.<sup>15</sup> Macrophages can be polarized to M1/M2 phenotypes according to the microenvironment, and M1 macrophages can lead to the copious secretion of proinflammatory cytokines such as interleukin 1 beta (IL-1 $\beta$ ), interleukin-6 (IL-6), interleukin-12 (IL-12), tumour necrosis factor alpha (TNF- $\alpha$ ), as well as the production of ROS and inducible nitric oxide synthase (iNOS).<sup>16</sup>

Tert-butylhydroquinone (tBHQ) is a synthetic phenolic antioxidant that has potent antioxidant activities.<sup>17</sup> Increasing evidence has demonstrated that tBHQ might potentially be applied for the treatment of oxidant stress-related diseases such as Alzheimer's disease,<sup>18</sup> ischaemic stroke,<sup>19</sup> and heart failure.<sup>20</sup> In addition, tBHQ could efficiently attenuate ROS production and inhibit the apoptosis of human neural stem cells.<sup>21</sup> However, the role of tBHQ in OA is unclear. Previous studies found that tBHQ had an anti-inflammatory effect both in vivo (10 to 100 mg/kg)<sup>22,23</sup> and in vitro (5 to 25  $\mu$ M).<sup>24</sup> Therefore, we selected similar concentration of tBHQ to explore its role in OA.

In this study, we demonstrated that tBHQ could efficiently alleviate destabilization of the medial meniscus (DMM)-induced OA through inhibiting apoptosis and inflammation of chondrocytes, and promoting differentiation of chondrocytes, as well as inhibiting ROS production and macrophage polarization by inhibiting activation of the NF- $\kappa$ B and MAPK signalling pathways. Our findings suggested that tBHQ might be an efficient therapeutic strategy for OA treatment.

## Methods

**Animals.** C57BL/6 female mice (ten-week-old) were housed under standard laboratory conditions (22°C (standard deviation (SD) 2), 40% to 60% humidity, 12 hr/12 hr light/dark cycle). According to body weight (20 g (SD 1)), a total of 36 mice were randomly divided into sham groups and DMM groups. Further, mice in the sham group were randomly divided into three sub-groups: sham group injected with PBS, sham group injected with 25 mg/kg tBHQ, and sham group injected with 50 mg/kg tBHQ. Mice in the DMM group were randomly divided into three sub-groups: DMM group injected with phosphate-buffered saline (PBS), DMM group injected with 25 mg/kg tBHQ, and DMM group injected with 50 mg/kg tBHQ. This made for a total of six groups, with six mice in each group. The animals were grouped by random number table. Overall, 36 mice were involved in the result analysis without any loss. The animal model with OA was induced by DMM as previously described.<sup>25</sup> One week after surgery, the mice were intraperitoneally injected with tBHQ (25 and 50 mg/kg) and observed for eight weeks. Mice in the control group received an equal volume of PBS. Finally, the mice were euthanized, and blood, plasma, and femur were collected for subsequent analysis. This study was approved by the Animal Ethics Committee of the First Affiliated Hospital of Guangzhou University of Traditional Chinese Medicine. All experimental procedures were carried out according to the recommendations of the National Council for Animal Care. We have included an ARRIVE checklist to show that we have conformed to the ARRIVE guidelines.

**Histopathological analysis.** Knee joint was isolated from each mouse and fixed in 10% paraformaldehyde and decalcified in 10 EDTA (pH = 7), and then embedded in

paraffin. Sections of 5  $\mu\text{m}$  thickness were used for histomorphometry. The sections were stained with Safranin O-fast green (SO) staining and each cartilage sample was stained with haematoxylin and eosin (H&E) following the manufacturer's instructions (Sigma-Aldrich, USA). Tissue samples were prepared for light microscopy using standard procedures. Histomorphometric analysis was performed using Image J (National Institutes of Health, USA). The scores of the femur and tibia were summed and presented as the Osteoarthritis Research Society International (OARSI) Score<sup>26,27</sup> for each sample as previously described.<sup>28</sup> All the sections were observed and scored in a blinded fashion.

**ELISA assay.** After the mice were euthanized, their blood samples were centrifuged at 2,000 rpm at 4°C for five minutes to obtain plasma samples. The expression of plasma IL-6, IL-1 $\beta$ , and TNF- $\alpha$  leptin was detected by enzyme-linked immunosorbent assay (ELISA) kit (Elabscience, China) following the manufacturer's instructions.

**MDA and SOD analysis.** The malondialdehyde (MDA) and superoxide dismutase (SOD) levels of blood were determined by MDA and SOD Assay Kit (Beyotime, China), respectively.

**Chondrocyte isolation and treatment.** Articular cartilage was isolated from femur head of mice, and chondrocytes were isolated as previously described.<sup>29</sup> In brief, mice were killed and disinfected in 75% alcohol for five minutes. The total articular cartilage was isolated from femur head and cut into pieces. Tissues were digested with 0.25% trypsin and 0.2% collagenase II for 40 minutes and four hours, respectively. Cells were then filtered through a 70- $\mu\text{m}$  cell strainer and washed three times with PBS. Afterward, the collected chondrocytes were seeded into culturing dishes in Dulbecco's Modified Eagle Medium (DMEM) medium at 37°C with 5% CO<sub>2</sub>. Culture medium was replaced every two to three days. The chondrocytes were used for subsequent experiments.

For the induction of inflammation and apoptosis, LPS (5 ng/ml, *Escherichia coli*, 055: B5, Sigma-Aldrich, USA) or IL-1 $\beta$  (10 ng/ml; Sigma-Aldrich) was added to the medium and incubated for 24 hours. Cells were then treated with different concentrations of tBHQ (10, 20, and 40  $\mu\text{M}$ ) for 12 hours, and collected for subsequent experiments.

**Western blot.** Total proteins were extracted using radioimmunoprecipitation assay (RIPA) lysis buffer as previously described.<sup>30</sup> Protein concentrations were determined using the protein assay kit (Beyotime, China). Protein samples (50  $\mu\text{g}$ ) were separated by 10% sodium dodecylsulphate (SDS)-polyacrylamide gels and electrotransferred to nitrocellulose membranes. After blocking in 3% bovine serum albumin (BSA) for one hour, the membranes were incubated with primary antibodies at 4°C for 12 hours. Primary antibodies (ratio 1:500) were:  $\beta$ -actin (sc-1616), Cleaved caspase-3 (9665), Cleaved caspase-9 (9509), Bax (14796), Bcl-2 (3498), p-IkBa (8219), IkBa (9245), p-P65 (3033), P65 (3032), p-ERK (4370), ERK (4695), p-JNK (9251), JNK (9252), p-P38 (9215), P38 (9212), p-STAT1 (9167), STAT1 (14994), p-STAT3 (9145),

and STAT3 (12640). After washing with TBST, the membranes were incubated with IgG-HRP at room temperature for one hour.  $\beta$ -actin was used as the internal reference. The protein signals were visualized using chemiluminescence detection (PerkinElmer Life Sciences, USA).

**qRT-PCR.** Total RNAs were extracted and purified using a RNeasy kit (Qiagen, Germany). RNA quality was checked by Nanodrop. Synthesis of complementary DNAs (cDNAs) from total RNAs (approximately 350 ng) was performed using the iscript cDNA synthesis kit (Takara, Japan). SYBR Green-based quantitative PCR was performed using the QuantStudio 6 Flex (Applied Biosystems, USA). Data were analyzed by 2<sup>- $\Delta\Delta\text{CT}$</sup>  method, and  $\beta$ -actin was used as the internal reference. The primers used were: IL-6: forward: 5'-GGCGGATCGGATGTTGTGAT-3', reverse: 5'-GGACCCAGACAATCGGTTG-3'; IL-1 $\beta$ : forward: 5'-AGTTGACGGACCCCAAAAG-3', reverse: 5'-TTTGAAGCTGGATGCTCTCAT-3'; TNF- $\alpha$ : forward: 5'-GGAACACGTCGGTGGATAATG-3', reverse: 5'-GGCAGACTTTGGATGCTTCTT-3'; MMP3: forward: 5'-GGCCTGGAACAGTCTTGGC-3', reverse: 5'-TGTCATC GTTCATCATCGTCA-3'; MMP13: forward: 5'-TGTTTGCA GAGCACTACTTCAA-3', reverse: 5'-CAGTCACCTCTAAGCC AAAGAAA-3'; Col2A1: forward: 5'-TGTTTGCA GAGCACTA CTTGAA-3', reverse: 5'-ACCAGGGGAACCACTCTCAC-3'; Col10a1: forward: 5'-GGGACCCCAAGGACCTAAAG-3', reverse: 5'-GCCCCAAGTACCTATCTCACCT-3'; Aggrecan: forward: 5'-CCACGACCCTCAAGAAGCTTTT-3', reverse: 5'-CTGCATCGTAGTGTCTCTTCG-3'; iNos: forward: 5'-CTCT TCGACGACCCAGAAAAC-3', reverse: 5'-CAAGGCCATGAA GTGAGGCTT-3'.

**ROS detection.** The intercellular ROS levels were detected by dichlorofluorescein (DCF) fluorescence as previously described.<sup>31</sup> Briefly, cells were treated by 5 ng/ml LPS for 24 hours and then treated with different concentrations of tBHQ (10, 20, and 40  $\mu\text{M}$ ) for another 12 hours. Subsequently, cells were incubated in 2.5  $\mu\text{M}$  DCF in DMEM at 37°C in the dark for 30 minutes. The ROS level was detected by flow cytometry. The mean fluorescence intensities for DCF were analyzed by Flow-Jo (BD FACSCalibur; BD Biosciences).

**Statistical analysis.** Data were presented as the mean and SD. Analyses were performed using GraphPad Prism 5 (USA). Difference among multiple groups was explored by one-way analysis of variance (ANOVA) followed by a post hoc test. A p-value < 0.05 was considered statistically significant.

## Results

**tBHQ attenuated cartilage destruction in DMM-induced OA mice.** To investigate the role of tBHQ in DMM-induced OA mice, the Sham-operated mice and DMM-induced mice were treated with different concentrations of tBHQ (25 and 50 mg/kg). We found that tBHQ had no obvious effect on Sham-operated mice, and tBHQ significantly depressed the cartilage destruction of DMM-induced mice in a dose-dependent manner (Figures 1a and 1b). It has

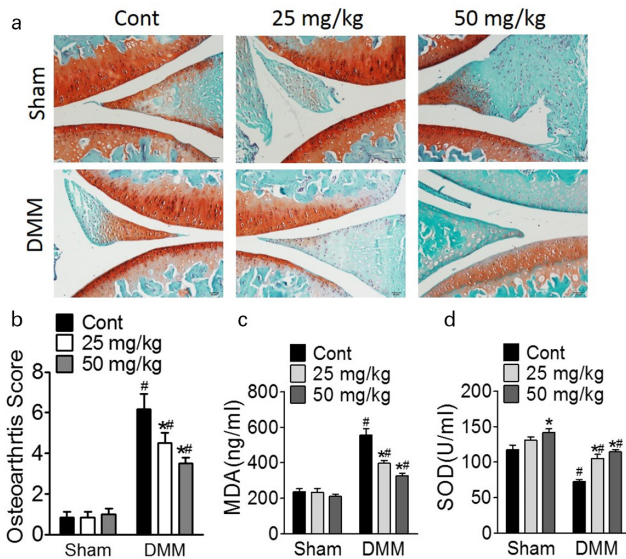


Fig. 1

Tert-butylhydroquinone (tBHQ) attenuated cartilage destruction in destabilization of the medial meniscus (DMM)-induced mice. After DMM surgery for one week, mice were intraperitoneally injected with different concentrations of tBHQ (25 and 50 mg/kg) and maintained for eight weeks. a) Representative images of Safranin O/fast green in knee joints and b) quantification of Osteoarthritis Research Society International (OARSI) score. Blood levels of c) malondialdehyde (MDA) and d) superoxide dismutase (SOD) in mice. N = 6 in each group. Differences among multiple groups were explored by one-way analysis of variance followed by a post hoc test. <sup>#</sup>p < 0.05 vs DMM-control group, <sup>##</sup>p < 0.05 vs Sham group with the same tBHQ treatment.

been reported that ROS plays an important role in OA development, which contains two aspects: oxidant stress and antioxidant reserves.<sup>32,33</sup> To further evaluate whether tBHQ inhibited DMM-induced OA progression through inhibiting ROS production, we detected the MDA level (an indicator of oxidant stress) and SOD activity (antioxidant reserves). The results showed that the levels of blood MDA exhibited no obvious change in Sham-operated mice after tBHQ administration, and the levels of blood MDA level in DMM-induced mice were remarkably decreased by tBHQ administration in a dose-dependent manner (Figure 1c). Meanwhile, tBHQ administration visibly increased the SOD activity in DMM-induced mice (Figure 1d). These results suggested that tBHQ could inhibit the development of DMM-induced OA in mice by suppressing ROS production.

**tBHQ inhibited IL-1 $\beta$ -induced chondrocyte apoptosis, inflammation, and differentiation in vitro.** In order to further explore the protective role of tBHQ against DMM-induced OA, we evaluated the role of tBHQ on chondrocyte apoptosis, inflammation, and differentiation. It has been reported that IL-1 $\beta$  can induce apoptosis and inflammation in chondrocytes, and meanwhile inhibits chondrocyte differentiation.<sup>34–36</sup> As shown in Figure 2a, IL-1 $\beta$  significantly increased the expression levels of apoptosis-related markers including Cleaved caspase-3, Cleaved caspase-9, and Bax, while it decreased the expression levels of Bcl-2; and tBHQ clearly decreased the expression levels of Cleaved

caspase-3, Cleaved caspase-9, and Bax, while increasing the expression levels of Bcl-2 (Figure 2a). Additionally, IL-1 $\beta$  visibly enhanced chondrocyte inflammation, which was characterized by elevated expression levels of cytokines such as IL-6 (Figure 2b), IL-1 $\beta$  (Figure 2c), TNF- $\alpha$  (Figure 2d), matrix metalloproteinase-3 (MMP-3) (Figure 2e), and MMP-13 (Figure 2f), while tBHQ visibly decreased the expression levels of these cytokines in a dose-dependent manner (Figures 2b to 2f). For chondrocyte differentiation, IL-1 $\beta$  distinctly inhibited the expression of chondrocyte differentiation-related proteins including collagen, type II, alpha 1 (Col2A1) (Figure 2g), collagen, type X, alpha 1 (Col10A1) (Figure 2h), and aggrecan, and tBHQ treatment notably attenuated IL-1 $\beta$ -induced decrease in differentiation-related markers including Col2A1, Col10A1, and aggrecan (Figures 2g to 2i). These results indicated that tBHQ could efficiently protect chondrocytes against IL-1 $\beta$ -induced damage in vitro.

**tBHQ decreased inflammation in DMM-induced mice in vivo.** Previous studies reported that inflammation of the joint can lead to several diseases including OA.<sup>37</sup> Based on the inhibitory inflammation of tBHQ in vitro, we further explored the role of tBHQ in DMM-induced mice in vivo. The results demonstrated that tBHQ had no obvious effect on the expression of inflammation-related markers including plasma IL-6, IL-1 $\beta$ , and TNF- $\alpha$  in Sham-operated mice, while tBHQ distinctly reduced the expression levels of plasma IL-6 (Figure 3a), IL-1 $\beta$  (Figure 3b), and TNF- $\alpha$  (Figure 3c) in DMM-induced mice in a dose-dependent manner. These results suggested that tBHQ could effectively inhibit DMM-induced inflammation in mice.

**tBHQ inhibited the activation of LPS-induced NF- $\kappa$ B and MAPK signalling pathways.** It has been reported that LPS can stimulate intracellular ROS production through activating the NF- $\kappa$ B and MAPK signalling pathways.<sup>38</sup> We found that LPS distinctly stimulated ROS production in vitro, and tBHQ markedly protected against LPS-induced ROS accumulation in a dose-dependent manner (Figure 4a). To explore whether tBHQ protected against LPS-induced ROS accumulation through inhibiting the NF- $\kappa$ B and MAPK signalling pathways, the phosphorylation level of NF- $\kappa$ B pathway members (p-I $\kappa$ B $\alpha$ , I $\kappa$ B $\alpha$ , p-p65, and p65) and MAPK signalling pathway members (p-ERK, ERK, p-JNK, JNK, p-p38, and p38) was detected. The results showed that LPS visibly activated the MAPK signalling pathway, which was characterized by increased expression levels of p-ERK, p-JNK, and p-p38, while tBHQ efficiently attenuated LPS-induced phosphorylation of p-ERK, p-JNK, and p-p38 (Figure 4b). Similarly, tBHQ also visibly attenuated LPS-induced phosphorylation of p-I $\kappa$ B $\alpha$  and p-p65, and increased the expression levels of I $\kappa$ B $\alpha$  (Figure 4c). Taken together, tBHQ could obviously protect against LPS-induced ROS accumulation by inhibiting the MAPK and NF- $\kappa$ B signalling pathways.

**tBHQ inhibited LPS-induced macrophage repolarization in vitro.** Synovial macrophage M1 polarization has been reported to exacerbate experimental OA progression.<sup>39</sup>

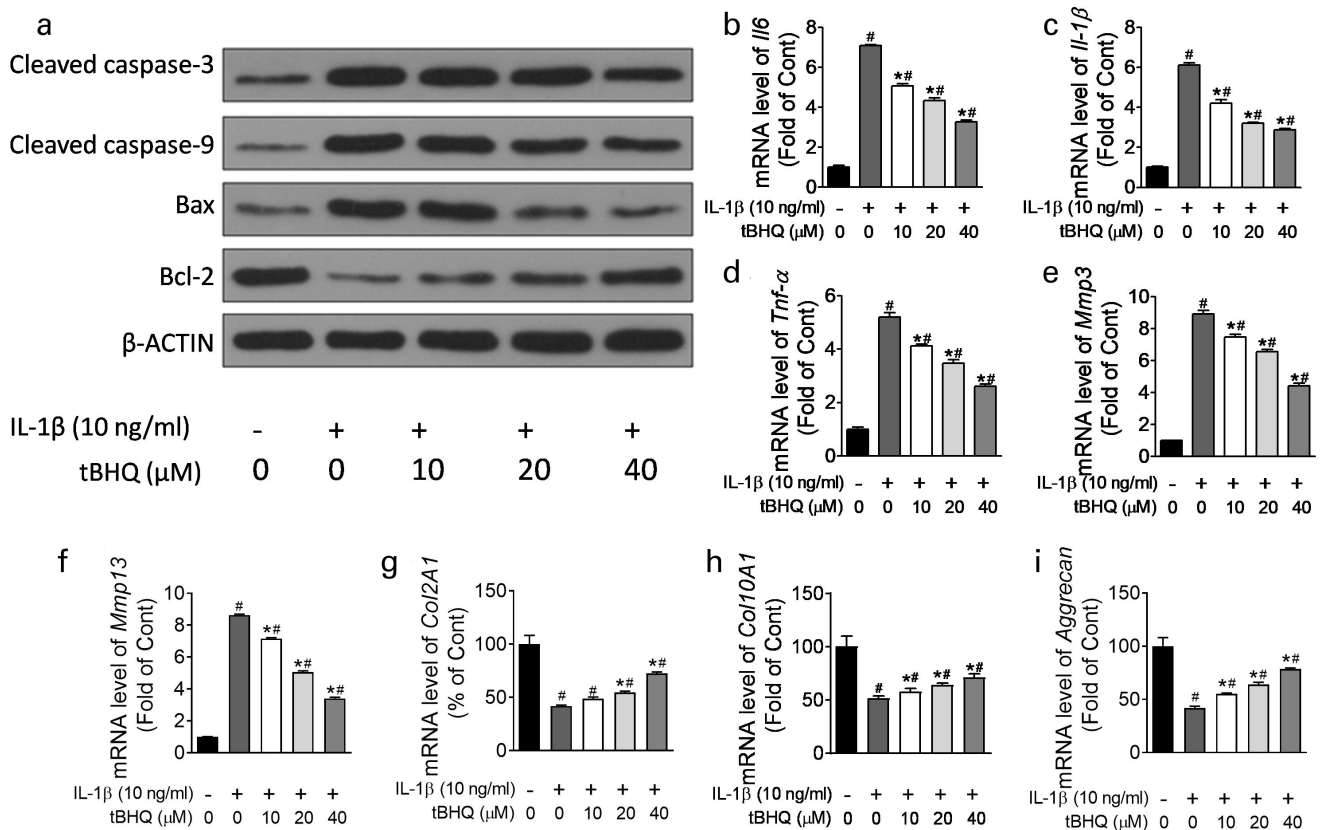


Fig. 2

Tert-butylhydroquinone (tBHQ) inhibited interleukin 1 beta (IL-1β)-induced chondrocyte apoptosis, inflammation, and differentiation in vitro. Chondrocytes were treated with 10 ng/ml IL-1β for 24 hours and then treated with different concentrations of tBHQ (10, 20, and 40 μM) for another 12 hours. b) to i) The expression levels of chondrocyte apoptosis-related markers including Cleaved caspase-3, Cleaved caspase-9, Bax, and Bcl-2 were detected by western blot. The expression levels of b) interleukin 6 (*IL-6*), c) *IL-1β*, d) tumour necrosis factor alpha (*TNF-α*), e) matrix metalloproteinase-3 (*MMP3*), f) *MMP13*, g) collagen, type II, alpha 1 (*Col2A1*), h) collagen, type X, alpha 1 (*Col10A1*), and i) *aggrecan* were measured by Real-time quantitative polymerase chain reaction (RT-qPCR). Each experiment was repeated three times. Difference among multiple groups was explored by one-way analysis of variance followed by a post hoc test. \**p* < 0.05 vs IL-1β treatment without tBHQ group; ##*p* < 0.05 vs control group without IL-1β and tBHQ. mRNA, messenger RNA.

To explore the role of tBHQ in macrophage repolarization, the expression levels of macrophage repolarization-related markers including p-STAT1, STAT1, p-STAT3, and STAT3 were detected. The results showed that LPS distinctly increased the expression levels of p-STAT1 and p-STAT3 in vitro, and tBHQ treatment notably attenuated LPS-induced STAT1 and STAT3 phosphorylation (Figure 5a). The expression levels of IL-6, IL-1β, TNF-α, and iNos were also detected, and it showed that tBHQ attenuated LPS-induced IL-6, IL-1β, TNF-α, and iNos elevation in a dose-dependent manner (Figure 5b). These results demonstrated that tBHQ could efficiently prevent against LPS-induced macrophage repolarization in vitro.

## Discussion

OA is a chronic, prevalent, debilitating joint disease characterized by progressive cartilage degradation, subchondral bone remodelling, bone marrow lesions, meniscal damage, and synovitis.<sup>40,41</sup> The molecular mechanisms underlying the progression of OA are still not fully understood, leading to a lack of effective treatment strategies.<sup>5</sup> A TGF-β1 receptor inhibitor, SB-505124, was

recently demonstrated to markedly attenuate articular cartilage degradation in an OA mouse model.<sup>42</sup> Parathyroid hormone-related protein shows potent antioxidant properties in osteoblastic cells that depend on its N-terminal and osteostatin domains, suggesting that it might serve as a potential therapeutic target for OA.<sup>43</sup> In addition, multiple intra-articular injections of allogenic bone marrow-derived stem cells can potentially attenuate knee lesions derived from surgically induced OA.<sup>44</sup> These findings indicate that potential therapeutic strategies for the treatment of OA are developing too slowly. Tert-butylhydroquinone has been identified to efficiently prevent multiple human diseases. For instance, it was reported that tBHQ can effectively attenuate neonatal hypoxic-ischaemic brain damage by activating Nrf2-mediated antioxidative signalling pathways.<sup>19</sup> Tert-butylhydroquinone can protect hepatocytes against lipotoxicity by inducing autophagy independently of Nrf2 activation.<sup>45</sup> Tert-butylhydroquinone promotes ischaemia-induced angiogenesis and improves heart functions in hypertensive rats by activating the AKT signalling pathway.<sup>46</sup> Tert-butylhydroquinone can also

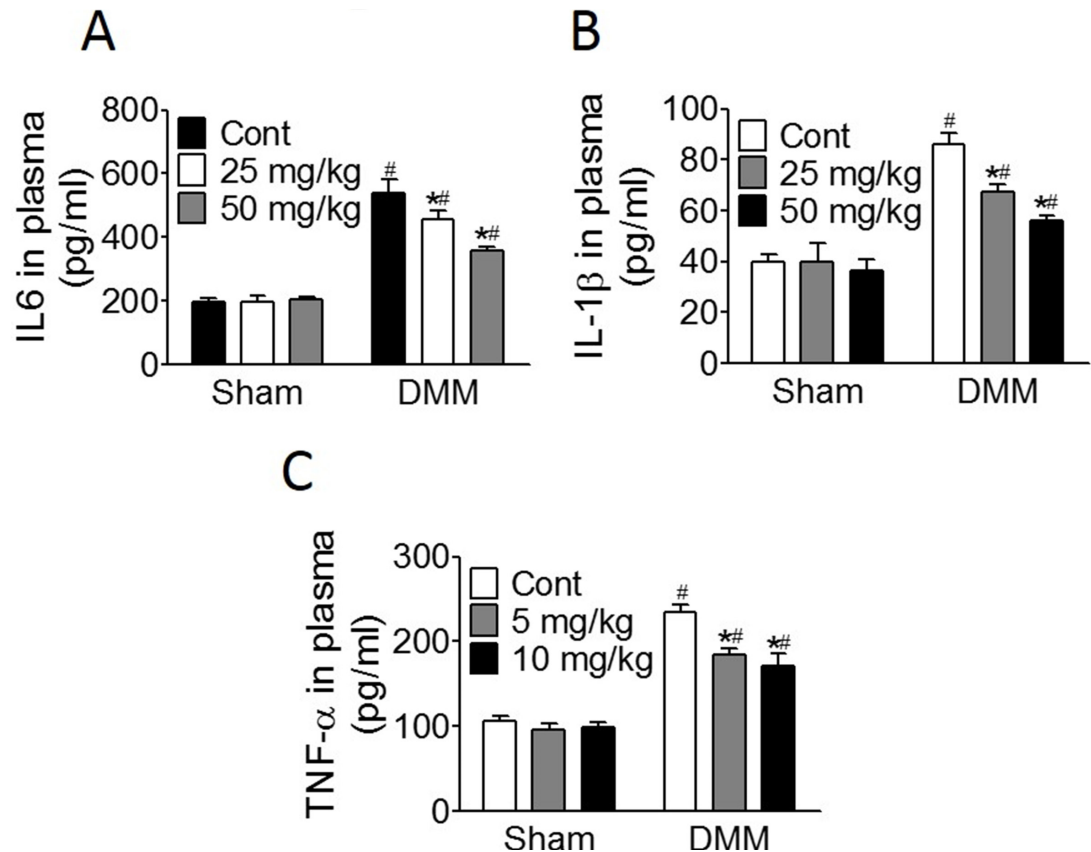


Fig. 3

Tert-butylhydroquinone (tBHQ) decreased destabilization of the medial meniscus (DMM)-induced inflammation *in vivo*. After DMM surgery for one week, mice were intraperitoneally injected with different concentrations of tBHQ (25 and 50 mg/kg) and maintained for eight weeks. The expression levels of a) interleukin 6 (IL-6), b) interleukin 1 beta (IL-1 $\beta$ ), and c) tumour necrosis factor alpha (TNF- $\alpha$ ) were detected by enzyme-linked immunosorbent assay (ELISA) assay. Difference among multiple groups was explored by one-way analysis of variance followed by a post hoc test. N = 6 in each group. \*p < 0.05 vs DMM-control group, #p < 0.05 vs Sham group with the same tBHQ treatment.

attenuate ethanol-caused apoptosis and activate Nrf2 antioxidant pathway in H9c2 cardiomyocytes.<sup>21</sup> Based on the important roles of tBHQ in ROS and cell apoptosis, we explored its potential role in OA in this study and demonstrated that tBHQ could efficiently alleviate cartilage destruction in DMM-induced OA mice. It could also inhibit ROS production by decreasing MDA level (an indicator of oxidant stress) and increasing SOD activity (antioxidant reserves). These results potentially indicated a protective effect of tBHQ on OA.

Apoptosis occurs in osteoarthritic cartilage and the relative contributions of chondrocyte apoptosis in the pathogenesis of OA are difficult to evaluate, and contradictory reports exist on the rate of apoptotic chondrocytes in osteoarthritic cartilage.<sup>13</sup> Recent findings indicate that OA is a much more complex disease with inflammatory mediators released by cartilage, bone, and synovium, and a source of inflammatory mediators implicated in the OA pain process and the degradation of the deep layer of cartilage.<sup>47</sup> In addition, a cartilage template is formed in which chondrocytes proliferate and differentiate into hypertrophic chondrocytes and are gradually replaced by bone, which is essential to

the development of OA.<sup>48</sup> To explore the role of tBHQ in the apoptosis, inflammation, and differentiation of chondrocytes, we selected IL-1 $\beta$  as the positive control that has been reported to significantly induce chondrocyte apoptosis and inflammation, while inhibiting the chondrocytes' differentiation *in vitro*.<sup>49–51</sup> Similar to the inhibitory effect of tBHQ in the cartilage destruction caused by DMM *in vivo*, we found that tBHQ could significantly inhibit IL-1 $\beta$ -induced chondrocyte apoptosis (apoptosis-related markers including Caspase-3, Cleaved caspase-9, Bax, and Bcl-2) and inflammation (cytokines such as IL-6, IL-1 $\beta$ , TNF- $\alpha$ , MMP-3, and MMP-13), and also significantly promote chondrocyte differentiation (chondrocyte differentiation-related markers including Col2A1, Col10A1, and aggrecan) *in vitro*. In addition, we detected the inflammatory level in DMM-induced mice and found that tBHQ could also significantly decrease the expression levels of cytokines such as IL-6, IL-1 $\beta$ , and TNF- $\alpha$  in DMM-induced mice *in vivo*.

In chondrocytes during OA, the elevated levels of ROS inhibit the PI3K/Akt pathway and activate the MEK/ERK pathway, therefore favouring the inflammatory process.<sup>52</sup> To determine the role of tBHQ on ROS

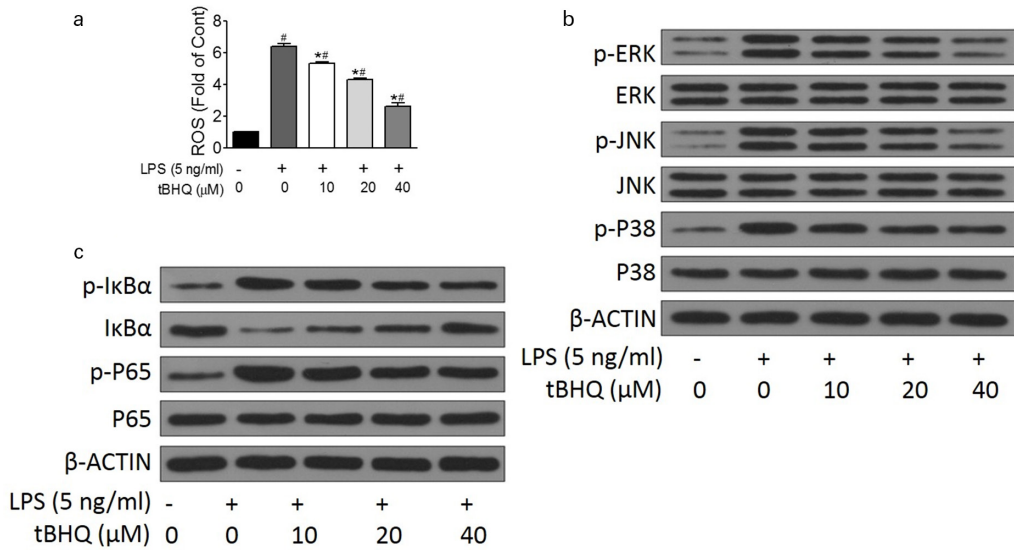


Fig. 4

Tert-butylhydroquinone (tBHQ) inhibited LPS-induced activation of NF- $\kappa$ B and MAPK signalling pathways. Chondrocytes were treated with LPS (5 ng/ml) for 24 hours and then treated with different concentrations of tBHQ (10, 20, and 40  $\mu$ M) for 12 hours. a) Reactive oxygen species (ROS) levels were detected by flow cytometry. b) The protein levels of p-ERK, ERK, p-JNK, JNK, p-P38, and P38 were detected by western blot. c) The protein levels of p-I $\kappa$ B $\alpha$ , I $\kappa$ B $\alpha$ , p-P65, and P65 were detected by western blot. Each experiment was repeated three times. Difference among multiple groups was explored by one-way analysis of variance followed by a post hoc test. \* $p < 0.05$  vs 5 ng/ml LPS group, # $p < 0.05$  vs control group without LPS and tBHQ.

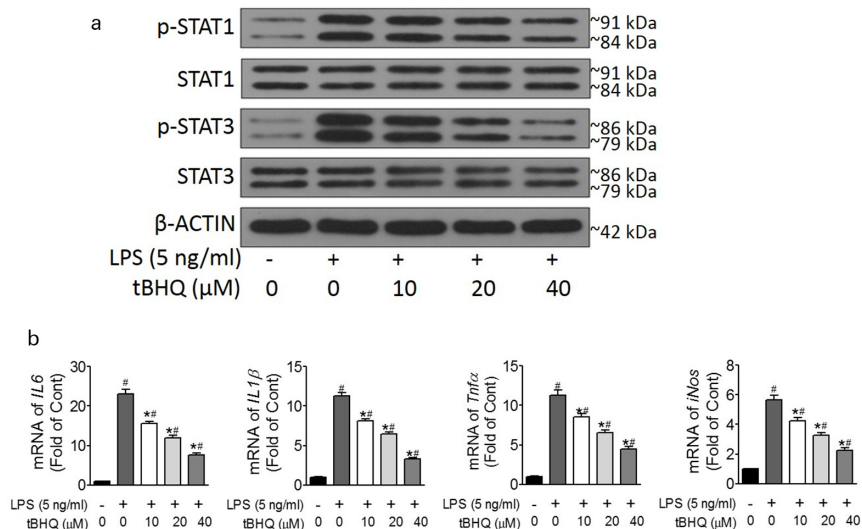


Fig. 5

Tert-butylhydroquinone (tBHQ) prevented destabilization of the medial meniscus (DMM)-induced macrophage repolarization in vitro. Chondrocytes were treated with LPS (5 ng/ml) for 24 hours and different concentrations of tBHQ (10, 20, and 40  $\mu$ M) for 12 hours. a) The protein levels of macrophage repolarization-related markers including p-STAT1, STAT1, p-STAT3, and STAT3 were detected by western blot. b) The messenger RNA (mRNA) expression levels of interleukin 6 (IL-6), IL-1 $\beta$ , tumour necrosis factor alpha (TNF- $\alpha$ ), and inducible nitric oxide synthase (iNOS) were detected by qRT-PCR. Each experiment was repeated three times. Difference among multiple groups was explored by one-way analysis of variance followed by a post hoc test. \* $p < 0.05$  vs 5 ng/ml LPS group, # $p < 0.05$  vs control group without LPS and tBHQ.

production, LPS was selected as the positive control which has been identified to stimulate ROS production.<sup>53</sup> The results demonstrated that tBHQ efficiently decreased LPS-stimulated ROS production. ROS has been shown to activate the MAPK and NF- $\kappa$ B pathways, leading to inflammatory responses.<sup>54</sup> p65 and I $\kappa$ B $\alpha$  are members of the NF- $\kappa$ B signalling pathway. When I $\kappa$ B $\alpha$  is phosphorylated and degraded, p65 is

activated through phosphorylation and transferred to nucleus from cytoplasm, and activates the transcription of downstream genes.<sup>55</sup> The MAPK signalling pathway mainly includes three members ERK, JNK, and p38, and phosphorylation of these can activate the MAPK signalling pathway.<sup>56</sup> Inhibition of ROS production has been reported to suppress the expression of inflammatory mediators in macrophages.<sup>57</sup> To further explore whether

tBHQ affected the activation of MAPK and NF- $\kappa$ B signaling pathways, we detected the phosphorylation levels of members in the MAPK and NF- $\kappa$ B pathways, and the results showed that tBHQ could significantly inhibit the activation of MAPK and NF- $\kappa$ B signalling pathways.

In the last few years, the concept of macrophage polarization and its role in inflammation has been recognized, which is clustered into two major macrophage polarization phenotypes: activated macrophages or M1, and alternatively activated macrophages or M2.<sup>58</sup> It has been reported that macrophage polarization plays important roles in bone metabolism<sup>59</sup> and associated simulation therapies.<sup>60</sup> It has also been reported that obesity aggravates knee OA by promoting infrapatellar fat pad (IFP) macrophage infiltration, M1 polarization, and the production of proinflammatory cytokines prior to the development of cartilage degeneration.<sup>61</sup> Further, Zhang et al<sup>39</sup> reported that synovial macrophage M1 polarization could exacerbate experimental OA partially through R-spondin-2. To explore the role of tBHQ in macrophage M1 polarization, we detected the phosphorylation levels of M1 polarization-related marker including STAT1 and STAT3, and demonstrated that tBHQ significantly decreased the phosphorylation levels of p-STAT1 and p-STAT3 induced by LPS, i.e. that tBHQ could effectively inhibit LPS-induced macrophage M1 polarization. Meanwhile, tBHQ also attenuated LPS-induced IL-6, IL-1 $\beta$ , TNF- $\alpha$ , and iNos elevation in vitro.

In conclusion, our results demonstrated that tBHQ could efficiently alleviate DMM-induced OA in vivo, and also protect chondrocytes against apoptosis, inflammation, and differentiation defects in vitro by inhibiting macrophage polarization and the activation of NF- $\kappa$ B and MAPK signalling pathways. Our study suggested that tBHQ might be an efficient therapeutic strategy for OA.

### Supplementary material



An ARRIVE checklist is included in the Supplementary Material to show that the ARRIVE guidelines were adhered to in this study.

### References

- Martel-Pelletier J, Barr AJ, Cicuttini FM, et al. Osteoarthritis. *Nat Rev Dis Primers*. 2016;2:16072.
- Nelson AE. Osteoarthritis year in review 2017: clinical. *Osteoarthr Cartil*. 2018;26(3):319–325.
- Felson DT. Clinical practice. Osteoarthritis of the knee. *N Engl J Med*. 2006;354(8):841–848.
- Li X, Yang Y, Sun G, et al. Promising targets and drugs in rheumatoid arthritis: A module-based and cumulatively scoring approach. *Bone Jt Res*. 2020;9:501–514.
- Krasnokutsky S, Samuels J, Abramson SB. Osteoarthritis in 2007. *Bull NYU Hosp Jt Dis*. 2007;65(3):222–228.
- Turrens JF. Mitochondrial formation of reactive oxygen species. *J Physiol (Lond)*. 2003;552(Pt 2):335–344.
- Collins JA, Diekman BO, Loeser RF. Targeting aging for disease modification in osteoarthritis. *Curr Opin Rheumatol*. 2018;30(1):101–107.
- Henrotin Y, Deby-Dupont G, Deby C, De Bruyn M, Lamy M, Franchimont P. Production of active oxygen species by isolated human chondrocytes. *Br J Rheumatol*. 1993;32(7):562–567.
- van Lent PL, Nabbe KC, Blom AB, et al. NADPH-oxidase-driven oxygen radical production determines chondrocyte death and partly regulates metalloproteinase-mediated cartilage matrix degradation during interferon-gamma-stimulated immune complex arthritis. *Arthritis Res Ther*. 2005;7(4):R885–95.
- Altindag O, Erel O, Aksoy N, Selek S, Celik H, Karaoglanoglu M. Increased oxidative stress and its relation with collagen metabolism in knee osteoarthritis. *Rheumatol Int*. 2007;27(4):339–344.
- Surapaneni KM, Venkataramana G. Status of lipid peroxidation, glutathione, ascorbic acid, vitamin E and antioxidant enzymes in patients with osteoarthritis. *Indian J Med Sci*. 2007;61(1):9–14.
- Ostalowska A, Birkner E, Wiecha M, et al. Lipid peroxidation and antioxidant enzymes in synovial fluid of patients with primary and secondary osteoarthritis of the knee joint. *Osteoarthr Cartil*. 2006;14(2):139–145.
- Hwang HS, Kim HA. Chondrocyte Apoptosis in the Pathogenesis of Osteoarthritis. *Int J Mol Sci*. 2015;16(11):26035–26054.
- Wang Y, Shen S, Li Z, Li W, Weng X. MIR-140-5p affects chondrocyte proliferation, apoptosis, and inflammation by targeting HMGB1 in osteoarthritis. *Inflamm Res*. 2020;69(1):63–73.
- Zhou F, Mei J, Han X, et al. Ginsenoside attenuates osteoarthritis by repolarizing macrophages through inactivating NF-kappaB/MAPK signaling and protecting chondrocytes. *Acta Pharm Sin B*. 2019;9(5):973–985.
- Ley K. The second touch hypothesis: T cell activation, homing and polarization. *F1000Res*. 2014;3:37.
- Li J, Bi Y, Yang H, Wang D. Antioxidative properties and interconversion of tert-butylhydroquinone and tert-butylquinone in soybean oils. *J Agric Food Chem*. 2017;65(48):10598–10603.
- Akhter H, Katre A, Li L, Liu X, Liu RM. Therapeutic potential and anti-amyloidosis mechanisms of tert-butylhydroquinone for Alzheimer's disease. *J Alzheimers Dis*. 2011;26(4):767–778.
- Zhang J, Tucker LD, Dong Y, et al. Tert-butylhydroquinone post-treatment attenuates neonatal hypoxic-ischemic brain damage in rats. *Neurochem Int*. 2018;116:1–12.
- Zhang Y, Fang Liu F, Bi X, Wang S, Wu X, Jiang F. The antioxidant compound tert-butylhydroquinone activates Akt in myocardium, suppresses apoptosis and ameliorates pressure overload-induced cardiac dysfunction. *Sci Rep*. 2015;5:13005.
- Shi X, Li Y, Hu J, Yu B. Tert-butylhydroquinone attenuates the ethanol-induced apoptosis of and activates the Nrf2 antioxidant defense pathway in H9c2 cardiomyocytes. *Int J Mol Med*. 2016;38(1):123–130.
- Hu B, Song J-T, Ji X-F, Liu Z-Q, Cong M-L, Liu D-X. Sodium ferulate protects against angiotensin II-induced cardiac hypertrophy in mice by regulating the MAPK/ERK and JNK pathways. *Biomed Res Int*. 2017;2017:3754942.
- Shintyapina AB, Vavilin VA, Safronova OG, Lyakhovich VV. The gene expression profile of a drug metabolism system and signal transduction pathways in the liver of mice treated with tert-butylhydroquinone or 3-(3'-tert-butyl-4'-hydroxyphenyl) propylthiosulfonate of sodium. *PLoS One*. 2017;12(5):e0176939.
- Lazaro I, Lopez-Sanz L, Bernal S, et al. Nrf2 activation provides atheroprotection in diabetic mice through concerted upregulation of antioxidant, anti-inflammatory, and autophagy mechanisms. *Front Pharmacol*. 2018;9:819.
- Glasson SS, Blanchet TJ, Morris EA. The surgical destabilization of the medial meniscus (DMM) model of osteoarthritis in the 129/SvEv mouse. *Osteoarthr Cartil*. 2007;15:1061–1069.
- Pritzker KP, Gay S, Jimenez SA, et al. Osteoarthritis cartilage histopathology: grading and staging. *Osteoarthr Cartil*. 2006;14(1):13–29.
- Wu J, Kuang L, Chen C, et al. Mir-100-5p-abundant exosomes derived from infrapatellar fat pad mscs protect articular cartilage and ameliorate gait abnormalities via inhibition of mtor in osteoarthritis. *Biomaterials*. 2019;206:S0142-9612(19)30166-8.
- Wang B-W, Jiang Y, Yao Z-L, Chen P-S, Yu B, Wang S-N. Aucubin protects chondrocytes against il-1 $\beta$ -induced apoptosis in vitro and inhibits osteoarthritis in mice model. *Drug Des Devel Ther*. 2019;13:3529–3538.
- Gosset M, Berenbaum F, Thirion S, Jacques C. Primary culture and phenotyping of murine chondrocytes. *Nat Protoc*. 2008;3(8):1253–1260.
- Wang KK, Posner A, Hajimohammadreza I. Total protein extraction from cultured cells for use in electrophoresis and western blotting. *BioTechniques*. 1996;20(4):662–668.
- Rastogi RP, Singh SP, Häder DP, Sinha RP. Detection of reactive oxygen species (ROS) by the oxidant-sensing probe 2',7'-dichlorodihydrofluorescein diacetate in the cyanobacterium *Anabaena variabilis* PCC 7937. *Biochem Biophys Res Commun*. 2010;397(3):603–607.
- Lepetos P, Papavassiliou AG. ROS/oxidative stress signaling in osteoarthritis. *Biochim Biophys Acta*. 2016;1862(4):576–591.



33. Banerjee AK, Mandal A, Chanda D, Chakraborti S. Oxidant, antioxidant and physical exercise. *Mol Cell Biochem*. 2003;253(1–2):307–312.
34. Kapoor M, Martel-Pelletier J, Lajeunesse D, Pelletier JP, Fahmi H. Role of proinflammatory cytokines in the pathophysiology of osteoarthritis. *Nat Rev Rheumatol*. 2011;7(1):33–42.
35. Shakibaei M, Allaway D, Nebrich S, Mobasher A. Botanical extracts from rosehip (*Rosa Canina*), willow bark (*Salix alba*), and nettle leaf (*Urtica dioica*) suppress IL-1 $\beta$ -induced NF- $\kappa$ B activation in canine articular chondrocytes. Evidence-based complementary and alternative medicine. *eCAM*. 2012;2012:509383.
36. Yu CD, Miao WH, Zhang YY, Zou MJ, Yan XF. Inhibition of Mir-126 protects chondrocytes from IL-1 $\beta$  induced inflammation via upregulation of bcl-2. *Bone Joint Res*. 2018;7(6):414–421.
37. Urban H, Little CB. The role of fat and inflammation in the pathogenesis and management of osteoarthritis. *Rheumatology*. 2018;57(suppl\_4):iv10–iv21.
38. Park J, Min JS, Kim B, et al. Mitochondrial ROS govern the LPS-induced pro-inflammatory response in microglia cells by regulating MAPK and NF- $\kappa$ B pathways. *Neurosci Lett*. 2015;584:191–196.
39. Zhang H, Lin C, Zeng C, et al. Synovial macrophage M1 polarisation exacerbates experimental osteoarthritis partially through R-spondin-2. *Ann Rheum Dis*. 2018;77(10):1524–1534.
40. McCulloch K, Litherland GJ, Rai TS. Cellular senescence in osteoarthritis pathology. *Aging Cell*. 2017;16(2):210–218.
41. Jayadev C, Hulley P, Swales C, et al. Synovial fluid fingerprinting in end-stage knee osteoarthritis: A novel biomarker concept. *Bone Joint Res*. 2020;9(9):623–632.
42. Zhang R-K, Li G-W, Zeng C, et al. Mechanical stress contributes to osteoarthritis development through the activation of transforming growth factor beta 1 (TGF- $\beta$ 1). *Bone Joint Res*. 2018;7(11):587–594.
43. Portal-Núñez S, Ardura JA, Lozano D, et al. Parathyroid hormone-related protein exhibits antioxidant features in osteoblastic cells through its N-terminal and osteostatin domains. *Bone Joint Res*. 2018;7(1):58–68.
44. Mahmoud EE, Adachi N, Mawas AS, Deie M, Ochi M. Multiple intra-articular injections of allogeneic bone marrow-derived stem cells potentially improve knee lesions resulting from surgically induced osteoarthritis: An animal study. *Bone Joint J*. 2019;101-B(7):824–831.
45. Li S, Li J, Shen C, et al. tert-Butylhydroquinone (tBHQ) protects hepatocytes against lipotoxicity via inducing autophagy independently of Nrf2 activation. *Biochim Biophys Acta*. 2014;1841(1):22–33.
46. Zhou NQ, Liu N, Li P, Ping S, Peng QS, Shi WD. Tert-butylhydroquinone promotes angiogenesis and improves heart functions in rats after myocardial infarction. *Clin Exp Hypertens*. 2017;39(5):402–408.
47. Berenbaum F. Osteoarthritis as an inflammatory disease (osteoarthritis is not osteoarthrosis!). *Osteoarthr Cartil*. 2013;21(1):16–21.
48. Wuelling M, Vortkamp A. Chondrocyte proliferation and differentiation. *Endocr Dev*. 2011;21:1–11.
49. Rao Z, Wang S, Wang J. Peroxiredoxin 4 inhibits IL-1 $\beta$ -induced chondrocyte apoptosis via PI3K/AKT signaling. *Biomed Pharmacother*. 2017;90:414–420.
50. Li Y, Wang J, Song X, et al. Effects of baicalin on IL-1 $\beta$ -induced inflammation and apoptosis in rat articular chondrocytes. *Oncotarget*. 2017;8(53):90781–90795.
51. Speichert S, Molotkov N, El Bagdadi K, Meurer A, Zaucke F, Jenei-Lanzl Z. Role of Norepinephrine in IL-1 $\beta$ -Induced Chondrocyte Dedifferentiation under Physioxia. *Int J Mol Sci*. 2019;20.
52. Yin W, Park JI, Loeser RF. Oxidative stress inhibits insulin-like growth factor-1 induction of chondrocyte proteoglycan synthesis through differential regulation of phosphatidylinositol 3-Kinase-Akt and MEK-ERK MAPK signaling pathways. *J Biol Chem*. 2009;284(46):31972–31981.
53. Cong Z, Ye G, Bian Z, Yu M, Zhong M. Jagged-1 attenuates LPS-induced apoptosis and ROS in rat intestinal epithelial cells. *Int J Clin Exp Pathol*. 2018;11(8):3994–4003.
54. Lee IT, Yang CM. Role of NADPH oxidase/ROS in pro-inflammatory mediators-induced airway and pulmonary diseases. *Biochem Pharmacol*. 2012;84(5):581–590.
55. Mendes AF, Carvalho AP, Caramona MM, Lopes MC. Role of nitric oxide in the activation of NF- $\kappa$ B, AP-1 and NOS II expression in articular chondrocytes. *Inflamm Res*. 2002;51(7):369–375.
56. Huang C, Jacobson K, Schaller MD. MAP kinases and cell migration. *J Cell Sci*. 2004;117(Pt 20):4619–4628.
57. Hsu HY, Wen MH. Lipopolysaccharide-mediated reactive oxygen species and signal transduction in the regulation of interleukin-1 gene expression. *J Biol Chem*. 2002;277(25):22131–22139.
58. Atri C, Guerfali FZ, Laouini D. Role of human macrophage polarization in inflammation during infectious diseases. *Int J Mol Sci*. 2018;19.
59. Nathan K, Lu LY, Lin T, et al. Precise immunomodulation of the M1 to M2 macrophage transition enhances mesenchymal stem cell osteogenesis and differs by sex. *Bone Joint Res*. 2019;8(10):481–488.
60. Heise G, Black CM, Smith R, Morrow BR, Mihalko WM. In vitro effects of macrophages on orthopaedic implant alloys and local release of metallic alloy components. *Bone Joint J*. 2020;102-B(7\_Suppl\_B):116–121.
61. Barboza E, Hudson J, Chang W-P, et al. Probiotic infrapatellar fat pad remodeling without M1 macrophage polarization precedes knee osteoarthritis in mice with diet-induced obesity. *Arthritis Rheumatol*. 2017;69(6):1221–1232.

#### Author information:

- H. Zhang, MD, Research Fellow
  - J. Li, DM, Research Fellow
  - X. Xiang, MD, Research Fellow
  - B. Zhou, DM, Research Fellow
  - C. Zhao, DM, Research Fellow
  - Q. Wei, DM, Research Fellow
  - Y. Sun, DM, Research Fellow
  - J. Chen, DM, Research Fellow
  - B. Lai, DM, Research Fellow
  - Z. Luo, DM, Research Fellow
  - A. Li, DM, Research Fellow
- Department of Orthopedics, The First Affiliated Hospital of Guangzhou University of Traditional Chinese Medicine, Guangzhou, China.

#### Author contributions:

- H. Zhang: Writing – original draft, Writing – review & editing.
- J. Li: Conceptualization, Writing – original draft.
- X. Xiang: Conceptualization.
- B. Zhou: Investigation.
- C. Zhao: Investigation.
- Q. Wei: Investigation.
- Y. Sun: Investigation.
- J. Chen: Investigation, Formal analysis.
- B. Lai: Formal analysis.
- Z. Luo: Writing – original draft.
- A. Li: Writing – original draft, Formal analysis.

#### Funding statement:

- This work was supported by the project of the National Natural Science Foundation of China (grant Nos. 81302994, 81473697, 81574002 and 81273778), GZUCM Science Fund for Creative Research Groups (grant No. 2016KYTD10), and GZUCM Torch Program (grant No. A1-AFD015142Z08). No benefits in any form have been received or will be received from a commercial party related directly or indirectly to the subject of this article.

#### Data sharing:

- The authors confirm that the open access funding for this study was covered by grants from the National Natural Science Foundation of China, GZUCM Science Fund for Creative Research Groups, and GZUCM Torch Program.

© 2021 Author(s) et al. This is an open-access article distributed under the terms of the Creative Commons Attribution Non-Commercial No Derivatives (CC BY-NC-ND 4.0) licence, which permits the copying and redistribution of the work only, and provided the original author and source are credited. See <https://creativecommons.org/licenses/by-nc-nd/4.0/>